Letter

Measurement of the electron affinity of lead and its isotope shifts

C. W. Walter, F. E. Vassallo, and N. D. Gibson
Department of Physics and Astronomy, Denison University, Granville, Ohio 43023, USA

(Received 24 January 2022; revised 9 June 2022; accepted 12 July 2022; published 26 July 2022)

The electron affinities of the primary isotopes of lead have been precisely measured using photodetachment threshold spectroscopy. The relative cross sections for photodetachment from Pb^- isotopes 206, 207, and 208 were observed using a tunable midinfrared optical parametric oscillator-amplifier to determine the ground-state binding energies. The isotope-averaged electron affinity of Pb was measured to be 356.723(7) meV, in excellent agreement with previous measurements. Furthermore, the isotope shifts in the electron affinities were determined to be −0.003(4) meV for ^{206}Pb − ^{208}Pb and −0.002(4) meV for ^{207}Pb − ^{208}Pb, providing insight to resolve previous discrepancies regarding the magnitude of these shifts.

DOI: 10.1103/PhysRevA.106.L010801

I. INTRODUCTION

Negative ions are important in a variety of physical processes, ranging from radiation absorption in the atmospheres of stars to plasmas and electrical discharges [1]. The electron affinity (EA) of an atom (equal to the binding energy of its negative ion) is an important thermochemical property that relates to an atom's ability to share electrons and form chemical bonds. Since the extra electron in a negative ion is not bound by a net Coulomb field, electron correlations and polarization are crucial for the stability and properties of negative ions [2,3]. Isotope shifts in electron affinities are sensitive to both electron correlations and interactions of the electrons and nucleus, providing new opportunities to better understand negative ions and complex atoms [4]. Thus, studies of negative ions and measurements of electron affinities and their isotope shifts yield key insights into the dynamics of multielectron interactions and serve as important tests of detailed atomic structure calculations.

As for the measurement of electron affinities, three experimental techniques have emerged as the primary high-precision methods: tunable laser photodetachment threshold spectroscopy (which is used in the present Letter) [5–9], slow electron velocity map imaging (SEVI) [10–13], and photodetachment microscopy [14–16]. The present Letter allows for direct comparison of these three techniques for the heavy and complex negative ion of lead ($Z = 82$), and it provides more precise information on the electron affinity shifts between its three primary isotopes (atomic masses 206, 207, and 208).

The lead negative ion has only one bound state, Pb^- ($6p^3\ ^4S^o_{3/2}$), which is formed by addition of a $6p$ electron to the ground state of the neutral atom, Pb ($6p^2\ ^3P_0$). Early traditional photoelectron spectrometry measurements by Feigerle *et al.* in 1981 yielded a value of 365(8) meV for the EA of Pb [17]. More recently in 2016, Chen and Ning used SEVI to obtain a much-higher-precision value of the EA for isotope 208 of 356.743(16) meV [12]. Subsequently in 2019, Bresteau *et al.* used photodetachment microscopy to measure the isotope-averaged EA, finding it to be 356.721(2) meV [16], a slightly lower and substantially more precise value than the SEVI result [12]. Notably, Chen and Ning also measured an unexpectedly large isotope shift in the binding energy of Pb^- to the Pb ($6p^2\ ^3P_2$) excited state for mass 206 relative to 208 of −0.40(18) cm^{-1} [−0.050(22) meV]. In contrast, Bresteau *et al.* estimated that the natural isotope dispersion for the electron affinity of Pb should probably not be larger than 0.02 cm^{-1} (0.0025 meV) based on a comparison to isotope shifts measured in transition energies of neutral Pb and Bi (which is isoelectronic to Pb^-) [16]. Clearly, further investigation of both the EA of lead and its isotope shifts is needed to resolve these discrepancies.

Theoretical calculations of the electron affinity of Pb are particularly challenging due to the complex correlations of the many valence and core electrons, as well as strong relativistic effects. A number of theoretical studies have been carried out over the past 50 years with increasing levels of sophistication (see Bresteau *et al.* for a summary of theoretical results prior to 2019 [16]). More recently in 2019, calculations by Finney and Peterson using a relativistic coupled-cluster-based Feller-Peterson-Dixon composite approach yielded a value of 367(22) meV for the EA of Pb [18], which is in good agreement with the experimental values albeit with much larger uncertainty. To our knowledge, no theoretical calculations of the isotope shifts in the Pb EA have been performed to date; however, theoretical studies of isotopes of other heavy, complex negative ions such as thallium have been very recently reported [19].

II. EXPERIMENTAL METHOD

In the present experiments, photodetachment threshold spectroscopy was used to measure the electron affinities of lead isotopes 206, 207, and 208. Photodetachment from Pb^- was observed as a function of photon energy using a crossed ion-beam–laser-beam system described previously [20,21]. Negative ions produced by a cesium sputter source [22] using a cathode packed with lead oxide and silver powder were

accelerated to 12.0 keV and mass selected using a 90° focusing sector magnet, giving typical single-isotope Pb^- currents of ≈10–100 pA. The ion beam was intersected perpendicularly by a pulsed laser beam, following which residual negative ions were electrostatically deflected into a Faraday cup, while neutral atoms produced by photodetachment continued undeflected to a multidynode detector. The neutral atom signal was normalized to the ion-beam current and the photon flux measured for each laser pulse. The spectra were obtained by repeatedly scanning the laser wavelength over a selected range and then sorting the data into photon energy bins of selectable width.

The laser system was an optical parametric oscillator (OPO)–optical parametric amplifier (OPA) (LaserVision) pumped by a 20-Hz Nd:YAG laser. In the present experiments, the OPA "idler" light with a bandwidth of ≈0.014 meV was used for photodetaching the Pb^- ions near the threshold wavelength of 3476 nm (356.7 meV). The wavelength of the midinfrared light was determined for each laser pulse using a procedure fully described previously [20]; briefly, a pulsed wave meter (High Finesse WS6-600) measured the wavelength of the OPO "signal" light, which was then used with the measured pump laser wavelength to determine the wavelength of the OPA light by conservation of energy. The laser beam diverges slightly as it leaves the OPA, so long focal length lenses were used to approximately collimate the beam. In the interaction region, the laser pulse had a typical energy of ≈50 μJ, pulse duration of ≈5 ns, and beam diameter of ≈0.25 cm.

As part of the present Letter, the crossing angle between the ion and laser beams was calibrated by measuring the photodetachment threshold of the O^- ($^2P_{1/2}$) excited state. This threshold has been accurately determined by Blondel *et al.* to be 1.439 158 5(22) [23], which is within the wavelength range of the OPO signal light. The laser-ion beam crossing angle was measured to be $89.0 \pm 0.3°$. The deviation of the crossing angle from 90° leads to a small Doppler shift of 2.2 μeV in the measured Pb^- threshold data acquired in the present experiment, which was accounted for in the analysis.

III. RESULTS AND DISCUSSION

The negative ion mass spectrum obtained with a PbO cathode showing the three primary isotopes of Pb^- at masses 206, 207, and 208 u is displayed in Fig. 1. Note that the minor isotope ^{204}Pb is also stable but, with a natural abundance of only 1.4% [24], its ion current is too small to investigate in the present Letter. The spectrum also shows a weak peak near mass 209 u; lead hydride negative ions are not expected to be produced by the sputter source [22], so this peak is likely $^{209}Bi^-$ due to recent use of bismuth in the ion source [25] and/or a small impurity of Bi in the PbO powder (note that Bi^- is produced much more efficiently by the sputter source than Pb^- [22]). The mass peaks in the measured spectrum were fit with Gaussians of a constant full width at half maximum of 0.48 u. The resolution of the system was determined to be $m/\Delta m \approx 400$; this high mass resolution was sufficient to select individual Pb^- isotopes for study. The Pb isotope fractions were measured to be $^{206}Pb^- : {}^{207}Pb^- : {}^{208}Pb^- = 0.27 : 0.24 : 0.49$, in good agreement with the ratios of

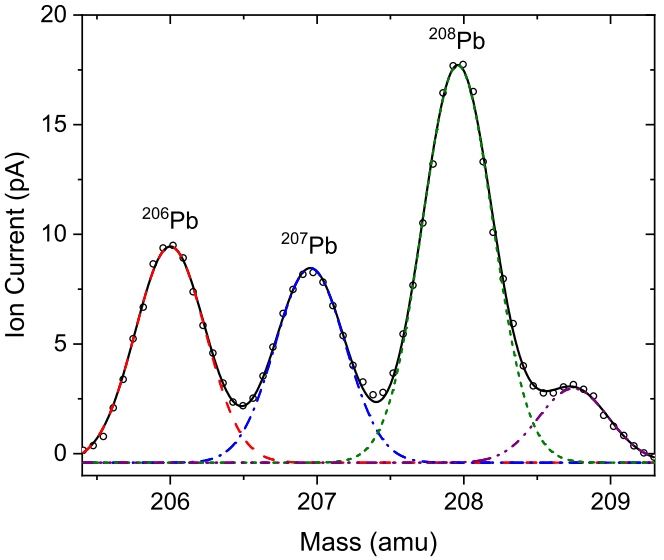

FIG. 1. Pb^- mass spectrum showing the three primary isotopes at masses 206, 207, and 208. The solid and dashed lines are fits to the observed peaks of Gaussians with fixed widths of 0.48 u. Also note the small additional peak near mass 209 which is likely due to $^{209}Bi^-$.

relative natural abundances of these three isotopes of 0.24 : 0.22 : 0.53 (excluding minor isotope 204) [24]. Importantly, the observed mass spectrum demonstrates that there was no significant cross contamination from other isotopes in the photodetachment spectra, as the adjacent isotopes are well separated.

Representative measured Pb^- photodetachment spectra near the threshold for detachment from the negative ion ground state Pb^- ($6p^3\ {}^4S^o_{3/2}$) to the neutral atom ground state Pb ($6p^2\ {}^3P_0$) are shown in Fig. 2 for each primary isotope. The spectra show near-zero background photodetachment signal below the threshold followed by a sharp rise in the cross section just above it. There is also a small tail in the data just before the threshold due to the bandwidth of the OPA of 0.014 meV. The minimum energy for detachment can be precisely determined from the data using the Wigner threshold law [26]. In the present case, a p electron is detached, so the cross section closely above threshold is dominated by s-wave detachment and increases as $(E - E_t)^{1/2}$, where E is the photon energy and E_t is the threshold energy. The Wigner s-wave function convoluted with the bandwidth of the OPA provides an excellent fit to the data, as shown in Fig. 2. The robustness of the fit was tested by trimming the range of data used in the fit, and no systematic deviation from the Wigner law was observed over the narrow range of the present measurements up to 0.15 meV above threshold. It should be noted that while including the bandwidth of the OPA improves the visual quality of the fit just below the threshold, essentially the same thresholds were obtained without inclusion of the bandwidth (within ≈ 1 μeV); this relative insensitivity to the assumed bandwidth of thresholds derived from Wigner law fits has been noted previously (see, for example, Bilodeau and Haugen [27]). The spectrum for each primary isotope of Pb^- was measured multiple times, and the weighted average

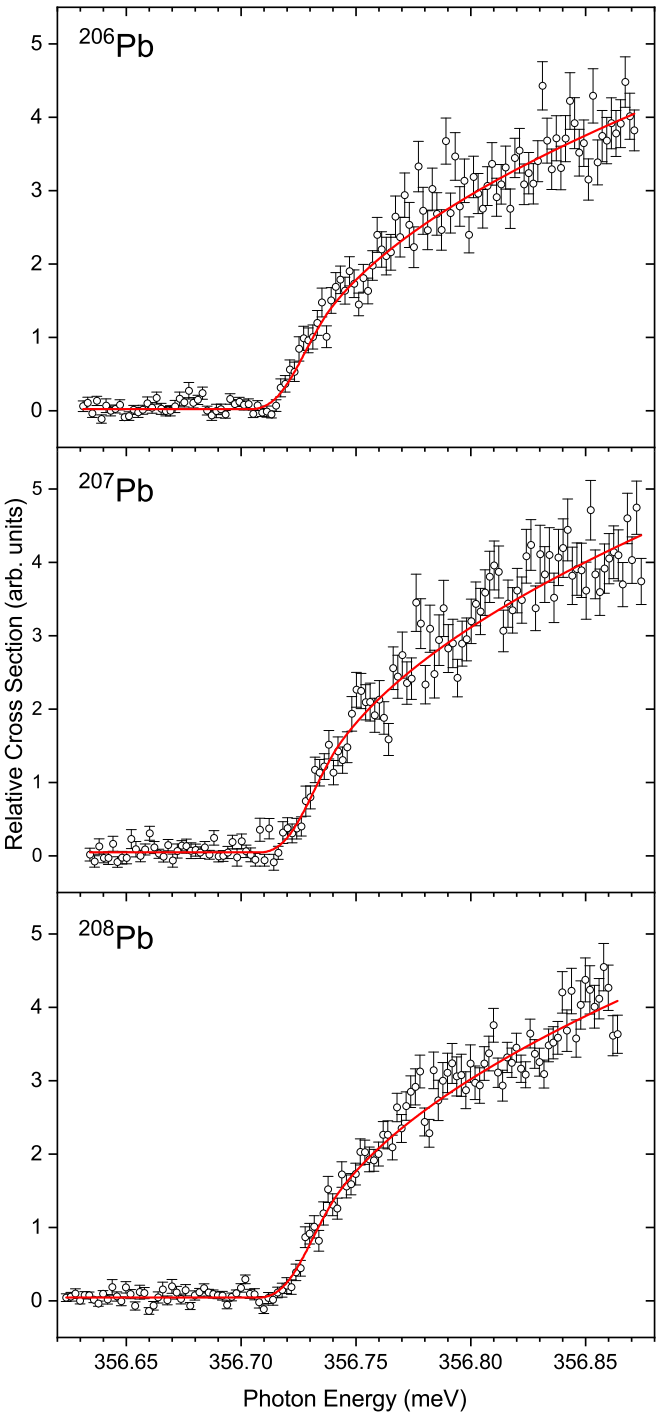

FIG. 2. Representative measured photodetachment spectra trials for different isotopes of Pb^- ($6p^3\ {}^4S^o_{3/2}$) near the threshold for detachment to ground state Pb ($6p^2\ {}^3P_0$); circles, data; line, s-wave Wigner law fit with the OPA linewidth of 0.014 meV included.

photodetachment threshold energies determined from the fits are listed in Table I. Figure 3 shows the fitted thresholds for the six trials performed on the most abundant isotope, ^{208}Pb.

The present measured EAs of Pb isotopes, equal to the binding energies of their negative ions, are for ^{206}Pb, ^{207}Pb, and ^{208}Pb, respectively: 356.721(7), 356.722(7), and 356.725(7) meV. These measured values yield an isotope-averaged EA based on the natural abundances of these isotopes of 356.723(7) meV. The quoted uncertainties represent full confidence intervals including both systematic and random contributions. The uncertainty in the absolute photon energy is estimated to be 3.5 μeV based on the absolute accuracy of the wave meter (2.5 μeV) plus a maximum calibration offset of 1 μeV determined by recent verification of the instrument with a stabilized HeNe laser. There is also a systematic uncertainty due to the 0.3° uncertainty of the laser-ion beam crossing angle, which gives an uncertainty in the Doppler shift of 0.7 μeV. The uncertainties associated with the photon energy and Doppler shift were added linearly yielding a systematic uncertainty of 4.2 μeV. Also note that in the present experiment any possible shift of the threshold due to the ponderomotive effect [28] is negligible because the laser beam is not focused, so the peak intensity of the laser pulse is relatively low ($\approx 5 \times 10^4$ W/cm^2), giving a shift of only $\approx$0.1 μeV [29]. The random uncertainty was calculated as twice the fitting uncertainty of the weighted average thresholds (giving statistical uncertainties of 1.0–1.6 μeV for different isotopes) added linearly with an uncertainty due to a small drift of the pump laser wavelength throughout individual data runs (measured to be less than 1 μeV). These factors yield a random uncertainty of 2.0–2.6 μeV for different isotopes. To obtain full confidence intervals, the systematic and random uncertainties were added linearly to determine the

TABLE I. Measured thresholds for photodetachment from Pb^- to ground state Pb ($^3P_0$) for different isotopes, with full confidence uncertainties in parentheses. The thresholds correspond to the electron affinities of the respective isotopes of Pb.

Isotope	Threshold (meV)
206	356.721(7)
207	356.722(7)
208	356.725(7)

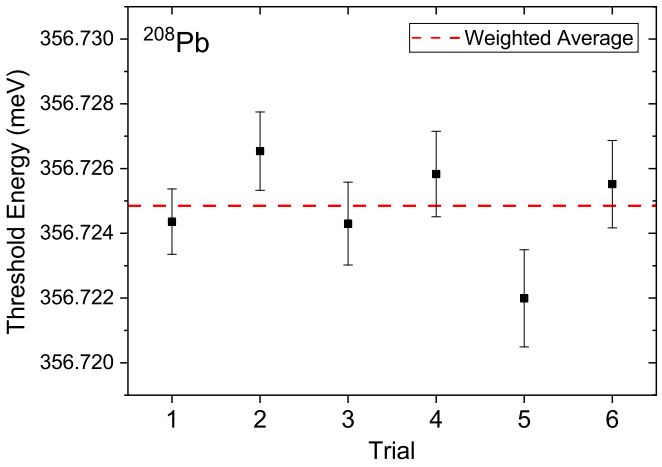

FIG. 3. Measured thresholds from different individual trials for photodetachment from the most abundant isotope, ^{208}Pb, shown by the square symbols with error bars indicating only statistical fitting uncertainties. The horizontal dashed line is the weighted average of the six trials.

TABLE II. Present results for the isotope-averaged electron affinity of Pb (including isotopes 206, 207, and 208 with their relative natural abundances), electron affinity of the most abundant isotope ^{208}Pb, and isotope shifts compared with previous results in meV. The isotope shifts measured in the present Letter are for binding energies of Pb^- relative to ground state Pb ($^3P_0$), while the isotope shifts measured by Chen and Ning [12] are for binding energies of Pb^- relative to the excited state Pb ($^3P_2$) (see text for further explanation).

Study	Isotope-averaged EA	EA ^{208}Pb	IS(206-208)	IS(207-208)
Present Letter	356.723(7)	356.725(7)	−0.003(4)	−0.002(4)
Bresteau *et al.* [16]	356.721(2)			
Chen and Ning [12]		356.743(16)	−0.050(22)	0.015(25)

total uncertainty for the isotope-specific and isotope-averaged EAs to be 7 μeV (rounded up).

It is worthwhile to also consider possible hyperfine effects for Pb and Pb^-. In the present experiments, the neutral atom state following photodetachment is Pb ($^3P_0$), so it has no hyperfine structure since $J = 0$. Isotopes ^{206}Pb and ^{208}Pb have no nuclear spin, thus their negative ions have no hyperfine structure. However, ^{207}Pb has nuclear spin $I = 1/2$, hence its negative ion state $^4S^o_{3/2}$ will be split into two hyperfine levels with $F = 1$ and 2. Therefore, photodetachment from $^{207}Pb^-$ to Pb ($^3P_0$) should yield two closely spaced thresholds separated by the hyperfine splitting of the negative ion. To our knowledge, there have not been any detailed theoretical calculations or experiments done on the hyperfine levels of $^{207}Pb^-$; however, Bresteau *et al.* estimated the hyperfine splitting to be about 732 MHz (0.003 meV) [16]. This splitting would be less than 1/4 of the bandwidth of the OPA used in the present experiments (≈0.014 meV), making it impossible to resolve the individual thresholds in this Letter. Furthermore, the measured photodetachment spectrum (Fig. 2) does not show any indication of hyperfine structure near the threshold. Consequently, the electron affinity reported here for ^{207}Pb should be considered a hyperfine-averaged value.

The isotope shifts of the electron affinities can be determined by subtracting the measured EAs of each isotope, e.g., IS(206-208) = EA(^{206}Pb) − EA(^{208}Pb). The shifts are found to be IS(206-208) = −0.003(4) meV and IS(207-208) = −0.002(4) meV (note that the quoted shifts are slightly different from direct subtraction of the values listed in Table I due to the round-off of those values for display). The uncertainties in the isotope shifts are smaller than the uncertainties in the individual EAs because of cancellation of the systematic effects, since the absolute photon energy calibration and the laser-ion beam crossing angle were the same for the different isotope measurements that were taken closely together in time. Therefore, the isotope shift uncertainty was calculated by adding in quadrature the random uncertainties of the individual EA values (2.0–2.6 μeV) to determine the uncertainty in their difference, which rounds up to 4 μeV.

The present results are compared with previous experimental results in Table II. The present isotope-averaged Pb EA of 356.723(7) meV is in excellent agreement with the value measured by Bresteau *et al.* using photodetachment microscopy of 356.721(2) meV [16], although our uncertainty is ≈3.5 times larger. Note that in both cases, the quoted uncertainties represent full confidence intervals. Our value of the EA for the most abundant isotope, mass 208, of 356.725(7) meV is in fair agreement with the value measured for this isotope by Chen and Ning using SEVI of 356.743(16) meV [12], but slightly lower.

Turning now to isotope shifts, the difference between our measured EAs for different Pb isotopes gives very small shifts of only −0.003(4) meV for IS(206-208) and −0.002(4) meV for IS(207-208). Although the precision available in the present experiments limits the uncertainty in the determination to about twice the observed shifts, these results still put an upper bound on the magnitude of the shifts and are consistent with the estimate made by Bresteau *et al.* that they should probably not be larger than 0.0025 meV [16]. Although there are not detailed theoretical calculations available yet for the isotopes of Pb^-, a very recent calculation has been reported for the isotope shift in the EA of the next lighter element, thallium (Z=81) [19]. In that work, Si *et al.* used multiconfiguration Dirac-Hartree-Fock and relativistic configuration interaction methods to calculate the shift in the EA between isotopes 203 and 205 of Tl to be −0.7014 GHz (−0.0029 meV) [19], which is very similar in magnitude to our measured Pb IS(206-208) of −0.003(4) meV.

While the isotope shifts measured in the present Letter are for the binding energies of Pb^- relative to ground state Pb ($^3P_0$), the isotope shifts measured by Chen and Ning [12] are for the binding energies of Pb^- relative to the excited state Pb ($^3P_2$). In order to compare their results to ours, it is also necessary to account for the isotope shifts in neutral Pb between the $^3P_2$ excited level and the $^3P_0$ ground state. As pointed out by Bresteau *et al.*, these values can be obtained from previous spectroscopic data for Pb transitions in the literature [30,31], yielding energy level shifts for Pb ($^3P_2$) of just 0.000 83(1) and 0.000 52(1) meV for isotopes 206 and 207 relative to 208, respectively [16]. These very small differences would only change the isotope shifts in the binding energies for Pb^- relative to Pb ($^3P_0$) compared to Pb ($^3P_2$) by less than 1 μeV. Regardless of whether this small effect is included, Chen and Ning's measured IS(207-208) of 0.015(25) meV [12] is consistent with our higher precision value of −0.002(4) meV, and both values are also consistent with Bresteau's estimate that the isotope shifts in the EA of Pb should probably not be larger than 0.0025 meV [16]. In contrast, Chen and Ning's IS(206-208) of −0.050(22) meV [12] is more than an order of magnitude larger than our value of −0.003(4) meV and much larger than Bresteau's estimate [16]. At this point, the reason for the unexpectedly large IS(206-208) obtained by Chen and Ning is not readily apparent.

IV. CONCLUSIONS

In summary, we have precisely determined the electron affinities of the three primary isotopes of lead (masses 206, 207, and 208) via the ground-state photodetachment thresholds of their negative ions. The present measured isotope-averaged electron affinity of 356.723(7) meV is in excellent agreement with the higher precision value previously measured by Bresteau *et al.* [16]. Furthermore, the isotope shifts in the electron affinity derived from the present experiments are −0.003(4) meV for IS(206-208) and −0.002(4) meV for IS(207-208); these values put useful upper bounds on the magnitudes of the shifts that are consistent with previous estimates for the shifts in the EA of Pb [16] and the calculated shift in the EA of the next lighter element, Tl [19]. It is hoped that the present results will spur further theoretical calculations of the electron affinity of Pb and other heavy negative ions, particularly targeting isotope effects.

ACKNOWLEDGMENTS

We thank C. Blondel for insightful correspondence and D. Burdick for technical assistance. This material is based upon work supported in part by the National Science Foundation under Grants No. PHY-1707743 and No. PHY-2110444. F.E.V. received partial support from the William G. and Mary Ellen Bowen Research Endowment at Denison University.

[1] D. J. Pegg, Rep. Prog. Phys. **67**, 857 (2004).
[2] C. F. Fischer, Phys. Scr. **40**, 25 (1989).
[3] T. Andersen, Phys. Rep. **394**, 157 (2004).
[4] T. Carette and M. R. Godefroid, Phys. Rev. A **89**, 052513 (2014).
[5] W. C. Lineberger and B. W. Woodward, Phys. Rev. Lett. **25**, 424 (1970).
[6] D. M. Neumark, K. R. Lykke, T. Andersen, and W. C. Lineberger, Phys. Rev. A **32**, 1890 (1985).
[7] M. Scheer, R. C. Bilodeau, C. A. Brodie, and H. K. Haugen, Phys. Rev. A **58**, 2844 (1998).
[8] P. Andersson, A. O. Lindahl, C. Alfredsson, L. Rogstrom, C. Diehl, D. J. Pegg, and D. Hanstorp, J. Phys. B **40**, 4097 (2007).
[9] C. W. Walter, N. D. Gibson, and S. E. Spielman, Phys. Rev. A **101**, 052511 (2020).
[10] A. Osterwalder, M. J. Nee, J. Zhou, and D. M. Neumark, J. Chem. Phys. **121**, 6317 (2004).
[11] D. M. Neumark, J. Phys. Chem. A **112**, 13287 (2008).
[12] X. Chen and C. Ning, J. Chem. Phys. **145**, 084303 (2016).
[13] R. Tang, R. Si, Z. Fei, X. Fu, Y. Lu, T. Brage, H. Liu, C. Chen, and C. Ning, Phys. Rev. Lett. **123**, 203002 (2019).
[14] C. Blondel, C. Delsart, and F. Dulieu, Phys. Rev. Lett. **77**, 3755 (1996).
[15] C. Valli, C. Blondel, and C. Delsart, Phys. Rev. A **59**, 3809 (1999).
[16] D. Bresteau, C. Drag, and C. Blondel, J. Phys. B **52**, 065001 (2019).
[17] C. S. Feigerle, R. R. Corderman, and W. C. Lineberger, J. Chem. Phys. **74**, 1513 (1981).
[18] B. A. Finney and K. A. Peterson, J. Chem. Phys. **151**, 024303 (2019); **151**, 159901(E) (2019).
[19] R. Si, S. Schiffmann, K. Wang, C. Y. Chen, and M. Godefroid, Phys. Rev. A **104**, 012802 (2021).
[20] C. W. Walter, N. D. Gibson, D. J. Carman, Y.-G. Li, and D. J. Matyas, Phys. Rev. A **82**, 032507 (2010).
[21] C. W. Walter, N. D. Gibson, Y.-G. Li, D. J. Matyas, R. M. Alton, S. E. Lou, R. L. Field, III, D. Hanstorp, L. Pan, and D. R. Beck, Phys. Rev. A **84**, 032514 (2011).
[22] R. Middleton, *A Negative-Ion Cookbook* (University of Pennsylvania, Philadelphia, 1990).
[23] C. Blondel, C. Delsart, and F. Goldfarb, J. Phys. B **34**, L281 (2001).
[24] M. Berglund and M. E. Wieser, Pure Appl. Chem. **83**, 397 (2011).
[25] C. W. Walter, S. E. Spielman, R. Ponce, N. D. Gibson, J. N. Yukich, C. Cheung, and M. S. Safronova, Phys. Rev. Lett. **126**, 083001 (2021).
[26] E. P. Wigner, Phys. Rev. **73**, 1002 (1948).
[27] R. C. Bilodeau and H. K. Haugen, Phys. Rev. A **64**, 024501 (2001).
[28] M. D. Davidson, J. Wals, H. G. Muller, and H. van Linden van den Heuvell, Phys. Rev. Lett. **71**, 2192 (1993).
[29] N. D. Gibson, C. W. Walter, C. Crocker, J. Wang, W. Nakayama, J. N. Yukich, E. Eliav, and U. Kaldor, Phys. Rev. A **100**, 052512 (2019).
[30] S. Bouazza, D. S. Gough, P. Hannaford, R. M. Lowe, and M. Wilson, Phys. Rev. A **63**, 012516 (2000).
[31] R. C. Thompson, M. Anselment, K. Bekk, S. Goring, A. Hanser, G. Meisel, H. Rebel, G. Schatz, and B. A. Brown, J. Phys. G **9**, 443 (1983).